



**HAL**  
open science

## Interactive buckling of an elastically restrained truss structure

Marcello Pignataro, Angelo Luongo

► **To cite this version:**

Marcello Pignataro, Angelo Luongo. Interactive buckling of an elastically restrained truss structure. Thin-Walled Structures, 1994, 19 (2-4), pp.197-210. hal-00802592

**HAL Id: hal-00802592**

**<https://hal.science/hal-00802592>**

Submitted on 20 Mar 2013

**HAL** is a multi-disciplinary open access archive for the deposit and dissemination of scientific research documents, whether they are published or not. The documents may come from teaching and research institutions in France or abroad, or from public or private research centers.

L'archive ouverte pluridisciplinaire **HAL**, est destinée au dépôt et à la diffusion de documents scientifiques de niveau recherche, publiés ou non, émanant des établissements d'enseignement et de recherche français ou étrangers, des laboratoires publics ou privés.

# Interactive Buckling of an Elastically Restrained Truss Structure

M. Pignataro

University of Roma 'La Sapienza', Faculty of Engineering, Department of Structural Engineering, Via Amatrice 10, I-Rome, Italy

&

A. Luongo

University of l'Aquila, Faculty of Engineering, Department of Structural Engineering, I-67040 Monteluco di Roio, L'Aquila, Italy

## ABSTRACT

*Interactive buckling of an elastically restrained truss structure is investigated by using an improved version of the Byskov–Hutchinson perturbation analysis. The mechanical model consists of two horizontal beams connected by rigid diagonals, whose out-of-plane displacements are prevented by a continuous distribution of linear springs. When the two horizontal beams are compressed, three buckling modes are possible: one overall in-plane mode and two local (lateral and torsional) modes which, for a particular choice of the geometry of the structure, may occur nearly simultaneously. Three nonlinear equilibrium equations are derived in the amplitudes of the three buckling modes and solved numerically for given initial imperfections.*

## 1 INTRODUCTION

The phenomenon of nonlinear buckling mode interaction has recently stimulated much interest in the literature. This is due to the fact that the post-critical behaviour of mechanical systems is strongly influenced

by the occurrence of simultaneous or nearly simultaneous buckling loads. Indeed, in such situations, structures are sensitive to initial imperfections and exhibit limit loads that are sometimes well below the bifurcation load.

This problem was first treated by Koiter<sup>1</sup> and subsequently has been investigated by many authors<sup>2-5,6,7,8 13</sup> who have solved a number of problems of technical interest by using a perturbation method. This method is particularly effective whenever several critical loads are coincident, in that it easily permits description of multiple bifurcations. If the critical loads are nearly coincident, the method is usually laborious<sup>14</sup> and sometimes even inapplicable in that it requires, for a correct description of the structure behaviour, the analysis of successive bifurcations along nonlinear post-critical paths. It is therefore often necessary to neglect small differences between buckling loads by making them coincident.

On the other hand, the Byskov–Hutchinson method,<sup>7</sup> extensively applied in the literature to the analysis of interactive buckling of thin-walled members, permits study of both simultaneous and nearly simultaneous buckling problems by furnishing the equilibrium paths of the systems directly. This method requires the solution of a sequence of constrained variational problems which furnish displacements of various orders as a function of the load; the load–displacement law is established at the end of the procedure through the solution of a system of nonlinear equations in the amplitude of interacting modes and loads. In this way, nonlinearities of the problem (quadratic, cubic, etc.) appear together in the final equilibrium equations, and not spread out at the various levels of perturbation analysis as in the Budiansky method. In the original version, however, this method requires the use of an iterative procedure related to the choice of the value of the  $\lambda_a$  load, by correspondence with which the perturbation equations are solved.

In this paper, the post-critical behaviour of a truss structure is analysed by using an improved version of the Byskov–Hutchinson method previously developed<sup>9</sup> which permits avoidance of the iterative procedure. The structure consists of two horizontal beams connected by rigid diagonals, whose out-of-plane displacements are prevented by a continuous distribution of linear springs. When the two beams are subjected to compressive forces, three buckling modes are possible which may occur nearly simultaneously and then interact in the post-critical range.

After determining the second-order displacement fields in closed form, three nonlinear equilibrium equations are derived in the amplitudes of the three buckling modes, accounting also for initial imperfections. By numerically solving these equations, the post-buckling equilibrium paths are obtained, and the influence of  $\lambda_a$  on the solution is investigated.

The system we wish to analyse in this section is illustrated in Fig. 1 and consists of two horizontal beams lying in the  $x$ - $y$  plane, connected by rigid diagonals, whose out-of-plane displacements are prevented by a continuous distribution of linear springs. The following assumptions are made:

- (i) the torsional rigidity of beams is negligible;
- (ii) the flexural curvatures of beams are linearised;
- (iii) the torsional curvature of beams is negligible;
- (iv) the axial strain in the beams is nonlinear;
- (v) the kinematic constraints due to diagonal beams are linearised.

The following kinematic relationships follow from hypothesis (v):

$$\begin{aligned}
 u_t(x) &= u(x) - hv'(x) & w_t(x) &= w(x) + h\theta(x) \\
 u_b(x) &= u(x) + hv'(x) & w_b(x) &= w(x) - h\theta(x) \\
 v_t(x) &= v_b(x) = v(x)
 \end{aligned}
 \tag{1}$$

where the symbols are illustrated in Fig. 1. The total potential energy of the system is then

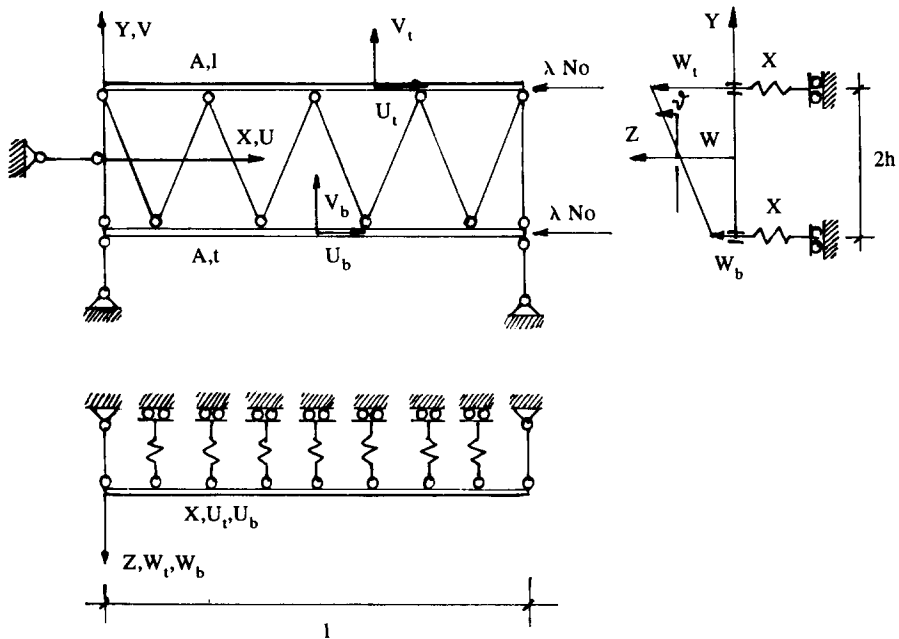


Fig. 1. Structural model.

$$\begin{aligned} \Phi = & \frac{1}{2} \int_0^l \left[ EA \left( u_t' + \frac{1}{2} v_t'^2 + \frac{1}{2} w_t'^2 \right)^2 + EI w_t''^2 + k w_t^2 \right] dx + \lambda N_0 u_t(l) \\ & + \frac{1}{2} \int_0^l \left[ EA \left( u_b' + \frac{1}{2} v_b'^2 + \frac{1}{2} w_b'^2 \right)^2 + EI w_b''^2 + k w_b^2 \right] dx + \lambda N_0 u_b(l) \end{aligned} \quad (2)$$

In eqn (2),  $EA$  and  $EI$  are the axial and bending stiffnesses of the beams, respectively,  $k$  is the stiffness per unit length of the springs,  $\lambda N_0$  is the axial load applied to the horizontal beams and a dash denotes differentiation with respect to  $x$ . By requesting the stationarity of eqn (2), the nonlinear equilibrium equations are obtained, which admit the following (nonunique) solution (fundamental path)

$$\begin{aligned} u_0(x) &= -\frac{\lambda N_0}{EA} x \\ v_0(x) &= w_0(x) = \theta_0(x) = 0 \end{aligned} \quad (3)$$

Let us now define the vector  $\mathbf{u} \equiv \{u, v, w, \theta\}$  and introduce the sliding variables  $\tilde{u}$  defined by  $u = u_0 + \tilde{u}$ ; then, accounting for eqn (3), we can write the equilibrium equations in the new variables as

$$\begin{aligned} EA \left( u' + \frac{1}{2} v'^2 + \frac{1}{2} w'^2 + \frac{1}{2} h^2 \theta'^2 \right)' &= 0 \\ EA h^2 v'''' + \lambda N_0 v'' - EA \left[ \left( u' + \frac{1}{2} v'^2 + \frac{1}{2} w'^2 + \frac{1}{2} h^2 \theta'^2 \right) v' \right]' & \\ - EA h^2 (\theta' w'')'' &= 0 \\ EI w'''' + \lambda N_0 w'' + k w - EA \left[ \left( u' + \frac{1}{2} v'^2 + \frac{1}{2} w'^2 + \frac{3}{2} h^2 \theta'^2 \right) w' \right]' & \quad (4) \\ + EA h^2 (v'' \theta')' &= 0 \\ EI \theta'''' + \lambda N_0 \theta'' + k \theta - EA \left[ \left( u' + \frac{1}{2} v'^2 + \frac{3}{2} w'^2 + \frac{1}{2} h^2 \theta'^2 \right) \theta' \right]' & \\ + EA h^2 (v'' w')' &= 0 \end{aligned}$$

with the boundary conditions

$$u(0) = 0 \quad v(0) = 0 \quad w(0) = 0 \quad \theta(0) = 0$$

$$v(l) = 0 \quad w(l) = 0 \quad \theta(l) = 0$$

$$EA \left[ u' + \frac{1}{2} v'^2 + \frac{1}{2} w'^2 + \frac{1}{2} h^2 \theta'^2 \right]_{x=l} = 0 \quad (5)$$

$$EAh^2[v'' - \theta'w']_{x=0,l} = 0$$

$$EI[w'']_{x=0,l} = 0 \quad EI[\theta'']_{x=0,l} = 0$$

where the tilde has been omitted.

The linear terms in eqns (4) furnish a linear eigenvalue problem which is assumed to admit  $m$  nearly coincident eigenvalues  $\lambda_i$  with the associated eigenvectors  $u_i$  ( $i = 1, \dots, m$ ). To study the nonlinear problem it is convenient to introduce the series expansion

$$u = \xi_i u_i + \xi_i \xi_j u_{ij} + \xi_i \xi_j \xi_k u_{ijk} + \dots \quad (i, j, k = 1, \dots, m) \quad (6)$$

where higher order displacement fields  $u_{ij}, u_{ijk}, \dots$  depend upon  $\lambda$ . Under suitable regularity conditions they can be expanded as

$$u_{ij} = u_{ij}^a + (\lambda - \lambda_a) u_{ij\lambda}^a + \dots \quad (7)$$

$$u_{ijk} = u_{ijk}^a + (\lambda - \lambda_a) u_{ijk}^a + \dots$$

around a starting point  $\lambda = \lambda_a$ . The numerical implications of the choice of  $\lambda_a$  will be discussed in the analysis of the results. By combining eqns (6) and (7), and substituting into eqns (4) and (5) and equating to zero terms with the same power of  $\xi$ , we obtain the following perturbation equations:  
*First order perturbation equations* (eigenvalue problem)

$$EAu_i'' = 0$$

$$EAh^2 v_i'''' + \lambda N_0 v_i'' = 0 \quad (8)$$

$$EIw_i'''' + \lambda N_0 w_i'' + kw_i = 0$$

$$EI\theta_i'''' + \lambda N_0 \theta_i'' + k\theta_i = 0$$

with the boundary conditions

$$u_i(0) = 0 \quad u_i'(l) = 0$$

$$v_i(0) = v_i(l) = 0 \quad v_i''(0) = v_i''(l) = 0$$

$$w_i(0) = w_i(l) = 0 \quad w_i''(0) = w_i''(l) = 0 \quad (9)$$

$$\theta_i(0) = \theta_i(l) = 0 \quad \theta_i''(0) = \theta_i''(l) = 0$$

*Second order perturbation equations*

$$\begin{aligned}
 EAu''_{ij} &= -\frac{EA}{2} (v'_i v'_j + w'_i w'_j + h^2 \theta'_i \theta'_j)' \\
 EAh^2 v''''_{ij} + \lambda_a N_0 v''_{ij} &= \frac{EAh^2}{2} (\theta'_i w'_j + \theta'_j w'_i)'' + \frac{EA}{2} (u'_i v'_j + u'_j v'_i)' \\
 EIw''''_{ij} + \lambda_a N_0 w''_{ij} + kw_{ij} &= \frac{EA}{2} (u'_i w'_j + u'_j w'_i - h^2 v''_i \theta'_j - h^2 v''_j \theta'_i)' \\
 EI\theta''''_{ij} + \lambda_a N_0 \theta''_{ij} + k\theta_{ij} &= \frac{EA}{2} (u'_i \theta'_j + u'_j \theta'_i - v''_i w'_j - v''_j w'_i)'
 \end{aligned} \tag{10}$$

with the associated boundary conditions

$$\begin{aligned}
 u_{ij}(0) &= 0 \\
 EA [2u'_{ij} + v'_i v'_j + w'_i w'_j + h^2 \theta'_i \theta'_j]_{x=l} &= 0 \\
 v_{ij}(0) = 0 \quad v_{ij}(l) &= 0 \\
 EAh^2 [2v''_{ij} - (\theta'_i w'_j + \theta'_j w'_i)]'_0 &= 0 \\
 w_{ij}(0) = w_{ij}(l) = 0 \quad w''_{ij}(0) = w''_{ij}(l) &= 0 \\
 \theta_{ij}(0) = \theta_{ij}(l) = 0 \quad \theta''_{ij}(0) = \theta''_{ij}(l) &= 0
 \end{aligned} \tag{11}$$

*Mixed second order perturbation equations*

$$\begin{aligned}
 EAu''_{ij\lambda} &= 0 \\
 EAh^2 v''''_{ij\lambda} + \lambda_a N_0 v''_{ij\lambda} &= -N_0 v''_{ij} \\
 EIw''''_{ij\lambda} + \lambda_a N_0 w''_{ij\lambda} + kw_{ij\lambda} &= -N_0 w''_{ij} \\
 EI\theta''''_{ij\lambda} + \lambda_a N_0 \theta''_{ij\lambda} + k\theta_{ij\lambda} &= -N_0 \theta''_{ij}
 \end{aligned} \tag{12}$$

with homogeneous boundary conditions identical to eqn (9).

Equations (10) and (12) represent a sequence of linear, ill-conditioned variational problems for  $\lambda_a$  near to the  $m$  eigenvalues  $\lambda_i$ , by correspondence with which the stiffness operator becomes singular. To eliminate this, it is necessary to introduce  $m$  auxiliary constraint conditions

$$Tu_{ij} = 0, \dots, Tu_{ij\lambda} = 0, \dots, Tu_l \delta u = 0 \quad (l = 1, \dots, m) \tag{13}$$

where  $T$  is a suitably chosen positive definite operator. In our analysis we take

$$Tu_1u_2 = 2N_0 \int_0^l (v'_1v'_2 + w'_1w'_2 + h^2\theta'_1\theta'_2) dx \quad (14)$$

and use the technique of the Lagrangian multipliers to enforce eqns (13).

Once the higher-order displacements have been determined, the nonlinear equilibrium equations in the displacements amplitude  $\xi_i$  have to be established. This can be accomplished by replacing eqns (6) into the virtual work principle  $\Phi'\delta u + \Psi'\delta u = 0$  where  $\Psi$  is the additional contribution to the energy deriving from initial imperfections. We then have

$$A_{il}\xi_i + A_{ijl}\xi_i\xi_j + A_{ijk}l\xi_i\xi_j\xi_k + C_{il}\bar{\xi}_i = 0 \quad (i, j, k, l = 1, \dots, m) \quad (15)$$

where the coefficients  $A$ ,  $C_{il}$  will be specified later and  $\bar{\xi}_i$  are the initial imperfection amplitudes.

### 3 THREE-MODE INTERACTION

The solution to differential equations (8), (10) and (12), and the evaluation of the coefficients of eqns (15), are performed in this section by assuming that three buckling modes may interact.

#### 3.1 Displacement fields

When the structure is subjected to compressive forces  $\lambda N_0$ , it buckles in three possible ways. The first consists of one half-wave deflection in the  $x$ - $y$  plane (overall buckling), defined by

$$u_1(x) = 0, \quad v_1(x) = a_1 \sin \frac{\pi x}{l}, \quad w_1(x) = 0, \quad \theta_1(x) = 0 \quad (16)$$

The associated critical load is

$$\lambda_1 = \frac{EAh^2}{N_0} \frac{\pi^2}{l^2} \quad (17)$$

whence  $\lambda_1 = 1$  if  $N_0 = EA h^2 \pi^2 / l^2$ . The second and third buckling modes consist of a multi-half-wave lateral and torsional deflection, respectively (local buckling). They are described by

$$u_2(x) = 0, \quad v_2(x) = 0, \quad w_2(x) = a_2 \sin \frac{n\pi x}{l}, \quad \theta_2(x) = 0 \quad (18)$$

$$u_3(x) = 0, \quad v_3(x) = 0, \quad w_3(x) = 0, \quad \theta_3(x) = a_3 \sin \frac{n\pi x}{l} \quad (19)$$



The associated (unique) buckling load multiplier is

$$\lambda_{2,3} \cong \left( n^2 \mu^2 + \frac{1}{n^2 \mu^2} \right) \frac{\sqrt{kEI}}{N_0} \quad (20)$$

where  $\mu = (\pi/l)^4 \sqrt{EI/k}$ . By normalizing according to

$$Tu^2 = e \quad (21)$$

where, for convenience, we take  $e = N_0 n^2 \pi^2 h^2 / l$ , we obtain

$$a_1 = nh, \quad a_2 = h, \quad a_3 = 1 \quad (22)$$

Consequently, from eqn (6), to within a first-order approximation, we get

$$\xi_1 = \frac{v_{1 \max}}{nh}, \quad \xi_2 = \frac{w_{2 \max}}{h}, \quad \xi_3 = \theta_{3 \max} \quad (23)$$

The higher-order displacement fields  $u_{ij}$ ,  $u_{ijz}$  are determined by solving the differential equations (10) and (12), respectively, with the associated boundary conditions. For the sake of brevity we do not show them here, since some of them have a cumbersome expression; we may state, however, that most of the components vanish except the following:  $u_{11}(x)$ ,  $u_{22}(x)$ ,  $u_{33}(x)$ ,  $v_{23}(x)$ ,  $w_{13}(x)$ ,  $\theta_{12}(x)$ ,  $v_{23z}(x)$ ,  $w_{13z}(x)$ ,  $\theta_{12z}(x)$ .

### 3.2 Nonlinear equilibrium equations

We are now in a position to write explicit expressions for the coefficients of the nonlinear equilibrium equations (15). By assuming  $m = 3$ , they are

$$A_{ii} = e(\lambda_i - \lambda) \quad (i = 1, 2, 3) \quad (\text{no sum with respect to } i) \quad (24)$$

$$A_{123} = -EAh^2 \int_0^l v_1' w_2' \theta_3' dx \quad (\text{symmetric with respect to indices}) \quad (25)$$

$$A_{1221} = A_{1122} = -4EAh^2 \left[ \int_0^l v_1' w_2' \theta_{12}' dx + (\lambda - \lambda_a) \int_0^l v_1' w_2' \theta_{12z}' dx \right] \quad (26)$$

$$A_{1331} = A_{1133} = -4EAh^2 \left[ \int_0^l v_1' \theta_3' w_{13}' dx + (\lambda - \lambda_a) \int_0^l v_1' \theta_3' w_{13z}' dx \right] \quad (27)$$

$$A_{2332} = A_{2233} = EAh^2 \left[ \int_0^l (2w_2'^2 \theta_3'^2 - 4w_2' \theta_3' v_{23}'') dx - 4(\lambda - \lambda_a) \int_0^l w_2' \theta_3' v_{23z}'' dx \right] \quad (28)$$

$$C_{ii} = -e\lambda_i \quad (i = 1, 2, 3) \quad (\text{no sum with respect to } i) \quad (29)$$

all other coefficients vanishing by  $e$ , we have the nonlinear equilibrium equations in the form

$$(\lambda - \lambda_1)\xi_1 + b\xi_2\xi_3 + c_{12}\xi_1\xi_2^2 + c_{13}\xi_1\xi_3^2 = -\lambda_1\bar{\xi}_1$$

$$(\lambda - \lambda_2)\xi_2 + b\xi_1\xi_3 + c_{12}\xi_1^2\xi_2 + c_{23}\xi_2\xi_3^2 = -\lambda_2\bar{\xi}_2$$

$$(\lambda - \lambda_3)\xi_3 + b\xi_1\xi_2 + c_{13}\xi_1^2\xi_3 + c_{23}\xi_2^2\xi_3 = -\lambda_3\bar{\xi}_3$$

where the following identifications have been made:  $b = A_{123}/e$ ,  $c_{12} = A_{1221}/e$ ,  $c_{13} = A_{1331}/e$ ,  $c_{23} = A_{2332}/e$ . For given imperfection amplitudes  $\bar{\xi}_i$ , eqns (30) are solved numerically.

### 3.3 Improved equilibrium equations

The coefficients of the nonlinear equilibrium equations appearing in eqns (15) are linear functions of  $\lambda$  because of the series expansion (7) of the higher-order displacement fields. This is apparent from their explicit expressions in the three-mode interaction problem (eqns (26)–(28)) just analysed. Such a dependence can be improved if higher-order displacements are more accurately evaluated as functions of  $\lambda$  without employing the linear approximation (7). To achieve this, the differential equations (10) have to be solved where  $\lambda_a$  is replaced by the generic  $\lambda$ .

If this procedure is applied to the truss-problem analysis performed in the previous section, the coefficients of eqns (26)–(28) have to be evaluated by taking the first integral only on the right-hand member, where the second-order displacements are now functions of  $\lambda$ .

## 4 NUMERICAL RESULTS

Numerical analysis has been performed on the truss beam having the following mechanical and geometrical properties:  $E = 2.06 \cdot 10^7 \text{ N/cm}^2$ ,  $A = 10 \text{ cm}^2$ ,  $I = 100 \text{ cm}^4$ ,  $k = 5.886 \text{ N/cm}^2$ ,  $l = 2500 \text{ cm}$ ,  $h = 25 \text{ cm}$ . By selecting for  $N_0$  the value of the overall critical load  $N_0 = 2.033 \cdot 10^5 \text{ N}$ ,  $\lambda_1 = 1.0$  follows. Since the local critical loads depend upon the number of half-waves  $n$ , we obtain from eqn (20)  $\lambda_{2,3} = 1.133$  for  $n = 5$ ,  $\lambda_{2,3} = 1.085$  for  $n = 6$  and  $\lambda_{2,3} = 1.158$  for  $n = 7$ . The lowest critical load is therefore that corresponding to  $n = 6$ . In the present analysis the interaction between local buckling modes associated with  $n = 6$  and the overall mode are considered; interactions with neighbouring buckling modes corresponding to  $n = 5$  and  $n = 7$  are ignored.

By solving eqns (10) and (12), higher-order displacements have been calculated. In particular, the displacement components  $v_{23}$ ,  $v_{23\lambda}$ ,  $w_{13}$ ,  $w_{13\lambda}$

have been plotted in Fig. 2. The  $\theta_{12}$  and  $\theta_{12z}$  components are not shown since they are proportional to  $w_{13}$  and  $w_{13z}$ , respectively, according to  $\theta_{12}(x) = w_{13}(x)/h$ ,  $\theta_{12z}(x) = w_{13z}(x)/h$ . Similarly the  $u_{ii}$  ( $i = 1, 2, 3$ ) components are not represented, since they have been eliminated in the definition of the coefficients of eqns (25)–(28). Second-order displacement fields in Fig. 2 have been calculated by correspondence with different values of  $\lambda_a$ . It is apparent that whereas the dependence of  $v_{23}$  on  $\lambda_a$  is very weak, in contrast such a dependence is notable for  $w_{13}$ . The explanation can be found in the analysis of the third of eqns (10) where we can see that, by putting  $i = 1$  and  $j = 3$ , the only nonvanishing known term  $(v_1''\theta_3)'$  is proportional to the sum of two sinusoids with wave-numbers  $n + 1$  and  $n - 1$ , respectively. Now, if we choose for  $\lambda_a$  the values of the critical load associated with  $n = 7$  or  $n = 5$ , the solution diverges since the known terms are proportional to the solution of the homogeneous equation.

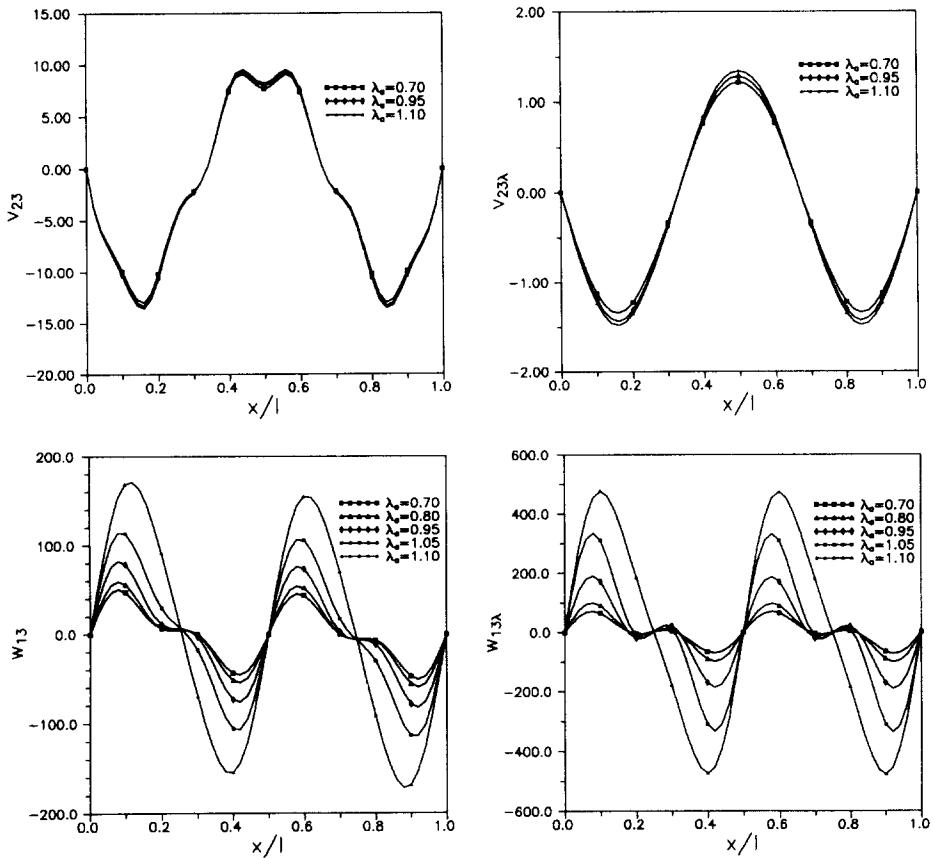


Fig. 2. Second-order and mixed second-order displacement fields for different values of  $\lambda_a$ .

Consequently  $w_{13}$  increases unboundedly when  $\lambda_a$  approaches one of these critical values.

It should be noted, in addition, that the dependence of  $w_{13}$  upon  $\lambda_a$  is strongly nonlinear, as can be argued by the presence of a nonunique  $w_{13\lambda}$  curve. This implies that the linear approximations (26)–(28) for the coefficients of eqns (30) may not be sufficiently accurate.

In order to evaluate the level of the discrepancies between the present analysis and a more accurate one, we plot the coefficient  $c_{13}(\lambda)$  evaluated as illustrated in Section 3.3 (Fig. 3(a)). It is seen that by correspondence with  $\lambda = 1.133$  (critical load associated with  $n = 5$ ) and  $\lambda = 1.158$  ( $n = 7$ ),  $c_{13}$  approaches infinity. This is not true for  $\lambda = 1$  ( $n = 1$ ) and  $\lambda = 1.085$  ( $n = 6$ ), since in these cases the orthogonality conditions (13) have been utilised in determining the higher-order displacement fields. This drawback would obviously disappear if we also included, among interacting modes, those corresponding to  $n = 5$  and  $n = 7$ . When this is not done,  $\lambda_a$  should be kept far away from these singular points. Figure 3(b) shows an enlargement of the previous figure around  $\lambda = 0.9$  where the exact curve  $c_{13}(\lambda)$  is compared with its linear approximation (eqn (27)).

Equations (30) have been solved numerically for given values of the initial imperfections. Initial imperfections in the shape of the overall buckling mode ( $\bar{\xi}_1 \neq 0, \bar{\xi}_2 = \bar{\xi}_3 = 0$ ) have been considered first and results are represented in Fig. 4(a) and (b) for  $\lambda_a = 0.70$  by taking the coefficients  $c_{ij}$  independent of  $\lambda$  as in Basu and Akhtar's<sup>2</sup> paper. In particular, Fig. 4(a) shows that the truss deflects initially in its own plane, then undergoes lateral-torsional buckling in which one of the two longitudinal beams

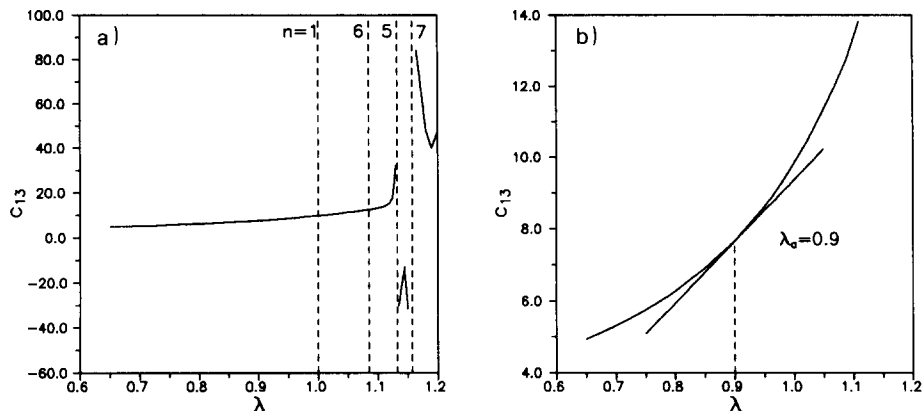


Fig. 3. Evaluation of the coefficient  $c_{13}$  (a) as a nonlinear function of  $\lambda$  and (b) as a linear approximation around  $\lambda_a = 0.9$ .

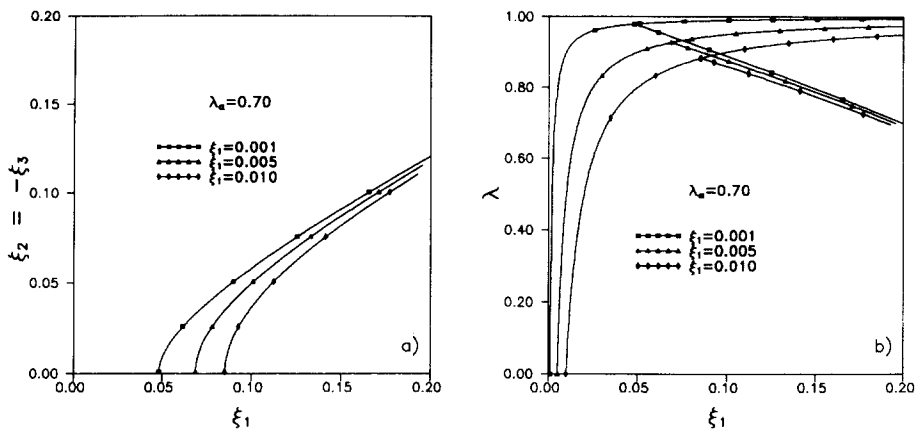


Fig. 4. Non-linear equilibrium paths of the truss with global imperfection.

remains in the initial plane. The bifurcation point depends upon the initial imperfections. In Fig. 4(b) the equilibrium curves  $\lambda$  as a function of  $\xi_1$  are shown.

If in addition, initial local imperfections are considered, the equilibrium paths are modified as shown in Fig. 5(a), where snapping points are manifested. These curves have been evaluated by considering again the coefficients  $c_{ij}$  in eqns (30) independent of  $\lambda$ . It is apparent that for the two different values of  $\lambda_a$  considered, the curves change remarkably. This spreading reduces when the  $c_{ij}$  coefficients are evaluated as linear functions of  $\lambda$  (Fig. 5(b)). If, in particular, attention is focused on the snapping points, we notice that, in the last case, they are nearly coincident.

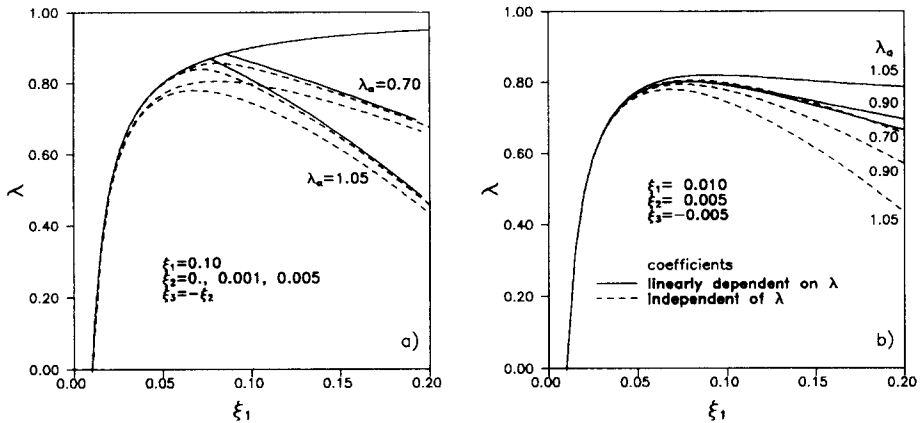


Fig. 5. Non-linear equilibrium paths of the truss with all types of imperfection. (a) Coefficients independent of  $\lambda$ , (b) coefficients linearly dependent upon  $\lambda$ .

Interactive buckling of an elastically restrained truss structure has been analysed. Three buckling modes, an overall and two local ones, are assumed to interact. A Galerkin type of approach has been employed, where the displacement fields are expressed as a series expansion in the unknown amplitudes, which includes higher-order displacement components. The dependence of these displacement components on the load  $\lambda$  is assumed linear around an appropriately selected starting point. The implications of this approximation, as well as that of the choice of the starting point, are discussed in the numerical applications. The system of three nonlinear equilibrium equations in the buckling mode amplitudes has been solved numerically for a number of values of initial imperfections.

The accuracy of the solution is investigated by comparing results achieved by assuming higher-order displacement fields independent of  $\lambda$  or linearly dependent upon  $\lambda$  and the improvement of the solution is highlighted.

## REFERENCES

1. Koiter, W. T., Over de stabiliteit van het elastisch evenwicht. PhD Thesis, H. J. Paris, Amsterdam, The Netherlands, 1945 (in Dutch); English Translation as NASA TT F-10, 833, 1957 and AFFDL Report TR 70-25, 1970.
2. Basu, P. K. & Akhtar, M. N., Interactive and local buckling of thin-walled members. *Thin-Walled Structures*, **12** (1991) 335-52.
3. Benito, R., Static and dynamic interactive buckling in plate assemblies. Doctoral dissertation, Washington Univ., St. Louis, USA, 1983.
4. Benito, R. & Sridharan, S., Mode interaction in thin-walled structural members. *J. Struct. Mech.*, **12**(4) (1984-85) 517-42.
5. Bradford, M. A. & Hancock, G. J., Elastic interaction of local and lateral buckling in beams. *Thin-Walled Structures*, **2** (1) (1984) 1-25.
6. Byskov, E., Damkilde, L. & Jonsen, K. J., Multimode interaction in axially stiffened cylindrical shells. *Mech. Struct. & Mach.*, **16**(3) (1988-89) 387-405.
7. Byskov, E. & Hutchinson, J. W., Mode interaction in axially stiffened cylindrical shells. *AIAA J.*, **15**(7) (1977) 941-8.
8. Luongo, A. & Pignataro, M., Multiple interaction and localization phenomenon in postbuckling of compressed thin-walled members. *AIAA J.*, **26**(11) (1989) 1395-1402.
9. Luongo, A. & Pignataro, M., Perturbation methods in the analysis of nonlinear interactive buckling. *Proc. AIMETA*, Pisa, Italy, 1990, pp. 45-50.
10. Luongo, A. & Pignataro, M., On the perturbation analysis of interactive buckling in nearly symmetric structures. *Int. J. Solids Struct.*, **23**(6) (1992) 721-33.

11. Menken, C. M., Groot, W. J. & Stallenberg, G. A. J., Interactive buckling of beams in bending. *Thin-Walled Structures*, **12** (1991) 415–34.
12. Pignataro, M. & Luongo, A., Asymmetric interactive buckling of thin-walled columns with initial imperfections. *Thin-Walled Structures*, **5** (1987) 365–86.
13. Sridharan, S. & Ali, M. A., Interactive buckling in thin-walled beam columns. *ASCE*, **111**(EM12) (1985) 1470–86.
14. Budiansky, B., Theory of buckling and postbuckling behaviour of elastic structures. *Advances in Applied Mechanics*, Vol. **14**, ed. Chia-Shun Yih. Academic Press, New York, USA, 1974, pp. 1–65.